Article

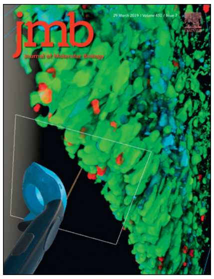

APOBEC3 Host Restriction Factors of HIV-1 Can Change the Template Switching Frequency of Reverse Transcriptase

Madison B. Adolph [1,2], Anjuman Ara [1,3] and Linda Chelico [1]

*1 - **Department of Biochemistry,** Microbiology, and Immunology, University of Saskatchewan, Saskatoon, Saskatchewan S7N 5E5, Canada*
*2 - **Department of Biochemistry,** Vanderbilt University, Nashville, TN 37232, USA*
*3 - **Saskatchewan Cancer Agency and Division of Oncology,** College of Medicine, University of Saskatchewan, Saskatoon, Saskatchewan S7N 5E5, Canada*

***Correspondence to Linda Chelico:** linda.chelico@usask.ca*
https://doi.org/10.1016/j.jmb.2019.02.015
Edited by Eric O. Freed

Abstract

The APOBEC3 family of deoxycytidine deaminases has the ability to restrict HIV-1 through deamination-dependent and deamination-independent mechanisms. Although the generation of mutations through deamination of cytosine to uracil in single-stranded HIV-1 (–) DNA is the dominant mechanism of restriction, the deaminase-independent mechanism additionally contributes. Previous observations indicate that APOBEC3 enzymes competitively bind the RNA template or reverse transcriptase (RT) and act as a roadblock to DNA polymerization. Here we studied how the deamination-independent inhibition of HIV-1 RT by APOBEC3C S188I, APOBEC3F, APOBEC3G, and APOBEC3H affected RT template switching. We found that APOBEC3F could promote template switching of RT, and this was dependent on the high affinity with which it bound nucleic acids, suggesting than an APOBEC3 "road-block" can force template switching. Our data demonstrate that the deamination-independent functions of APOBEC3 enzymes extend beyond only disrupting RT DNA polymerization. Since alterations to the RT template switching frequency can result in insertions or deletions, our data support a model in which APOBEC3 enzymes use multiple mechanisms to increase the probability of generating a mutated and nonfunctional virus in addition to cytosine deamination.

Introduction

The APOBEC3 (A3) deoxycytidine deaminases are a family of host restriction factors for retroviruses, retrotransposons, and endogenous retroviruses [1,2]. The A3 enzymes are well characterized for restricting replication of the human immunodeficiency virus-1 (HIV-1; referred to as HIV) [3]. For A3-mediated HIV restriction to occur, the A3 enzymes must become virion encapsidated [4]. The HIV protein Vif induces the polyubiquitination and degradation of A3 enzymes preventing their encapsidation. However, degradation of A3 enzymes is not complete, and some A3s can become encapsidated at a low amount into virions in the presence of Vif [5,6]. HIV restriction is primarily mediated by the deamination of cytosine (C) to uracil (U) on single-stranded (ss) DNA during synthesis of (–) HIV DNA after virus entry into a target cell [7,8]. These deaminations lead to guanine (G)-to-adenine (A) hypermutation of the virus genome when uracil is used as a template during HIV reverse transcription [9–11]. The G-to-A hypermutation leads to inactivation of the provirus [9–11] or if mutagenesis does not reach sufficient levels, A3 activity can result in viral evolution in the form of drug resistance or CTL escape [12–16]. Of the seven human A3 deaminases, A3G, A3F, A3D, and A3H (haplotypes II, V, and VII) are able to restrict replication of HIV to varying degrees [1,3,17]. In addition, a human polymorphism of A3C (I188) has HIV restriction activity, while the more common S188 polymorphism of A3C does not [18,19].

A3 enzymes are ssDNA deaminases, thereby necessitating that the RNase H domain of reverse transcriptase (RT) degrades the RNA template, which leaves regions of ssDNA available for deamination by A3 [8,20]. Since these ssDNA regions are only available for a limited amount of time, A3 enzymes must possess efficient ssDNA scanning mechanisms and scan the template processively in order to locate target cytosines. The processive action is mediated through facilitated diffusion, which includes both one-dimensional sliding and three-dimensional translocations such as jumping and intersegmental transfer [21,22]. A3 enzymes that scan ssDNA processively and are able to use a combination of one-dimensional and three-dimensional movements induce higher mutational loads than non-processive A3s [6,18,23,24]. In addition, certain A3s are able to inhibit HIV through deamination-independent mechanisms that act in concert with the deamination activity [25–34]. A3G and A3F delay the initiation of primer extension, decrease processivity, and inhibit DNA elongation by HIV RT to varying degrees by binding to the RNA template and acting as a physical block to the scanning mechanism of RT [25,27,28,32,35]. A3G also binds directly with RT to cause these disruptions of DNA synthesis [25,34]. Although the deamination-dependent effects of A3 enzymes are the dominant form of HIV restriction, there are cumulative effects of the deamination-independent restriction that effect viral infectivity [25,34,36]. Notably, although the restriction of HIV by human A3 enzymes is a combination of deamination-dependent and deamination-independent mechanisms, the mouse A3 enzyme can inhibit Moloney Murine Leukemia Virus RT in the absence of any deamination, suggesting that for some A3 and retrovirus relationships, deoxycytidine deaminase activity is dispensable [37].

Since the dominant mechanism of HIV-1 restriction by A3 enzymes is deamination, the deamination-independent mode of restriction has remained poorly characterized. Namely, no studies to date have examined if the physical inhibition of RT-mediated DNA synthesis has other effects on RT activity, such as template switching. During reverse transcription, RT undergoes two separate template-switching events that are necessary to complete synthesis of (+) DNA [38–40]. It has been suggested that the low template affinity and low processivity of RT are advantageous because it allows for template-switching events to occur that are essential to produce the proviral DNA. These events include first-strand transfer of the minus strand (–) strong-stop DNA to the 3′ end of the genome in order for (–) DNA synthesis to proceed further [38–40]. However, RT can also switch templates at other random locations in a homology directed fashion, and this can create diverse retroviral populations if the switch occurs between distinct templates (intermolecular switch) [41–44] or lead to deletions of genomic regions if the switch occurs on the same RNA molecule (intramolecular switch) [45,46]. Template switching occurs optimally when the equilibrium between polymerization and RNase H degradation is maintained (Fig. 1a, left). Aberrant template switching can occur with “slow polymerase” mutants that disrupt this balance (Fig. 1a, middle) [47]. Notably, amplification of near-full-length proviral genomes from HIV+ individuals showed that even within the first few weeks of infection, defective proviruses accumulated and accounted for over 90% of the total proviral genomes [48]. These defective viruses arose from a combination of deletions that presumably resulted from RT template switching, RT error, and A3-induced stop codons [48]. Recently, a study showed that blocking RT template switching resulted in reduced viral titers and proviruses that contained large deletions [49]. Since template switching is a major mechanism for HIV to maintain genomic integrity and evolve new recombinant forms [49,50], the deletions may be a consequence of the obligatory template switching events or may be due to encountered blocks on the primer/template.

We hypothesized that if an A3 inhibited RT-mediated DNA polymerization either through a “roadblock” by binding the primer/template or a direct interaction with RT [26,33,34], it may also facilitate the dissociation of RT from the template and effect template switching (Fig. 1a, right). To test this hypothesis, we examined A3s with the strongest HIV restriction ability, A3G, A3F, A3H haplotype II (referred to as A3H), and a recently characterized A3C I188 variant [19,51,52]. Our data demonstrate that depending on the nucleic acid binding affinity of the A3, the template switching of RT can be increased, decreased, or unaffected by A3 enzymes. Either increases or decreases in template switching could increase the probability of generating a mutated and nonfunctional virus independent of cytosine deamination, suggesting that A3 enzymes have a previously underestimated multi-pronged approach to restricting HIV.

Results

Modulation of HIV RT template switching by A3 enzymes

We examined the ability of RT to undergo template switching *in vitro* in the presence of varying amounts of an A3. The RNA template was generated by cloning a region of the HIV genome into a vector that enabled *in vitro* transcription with T7 RNA Polymerase. The resulting RNA contained the primer binding site (PBS), and an 18-nucleotide (nt) RNA primer was annealed to the PBS to generate the primer/template (p/t) (Fig. 1b and see Materials and Methods). This “donor region” was used because synthesis of DNA by RT in this region is known to be sensitive to A3 interference due to the inefficient initiation of DNA synthesis of RT from an RNA primer [25,53,54]. We also used an “acceptor” template that did not contain the PBS, but did contain a 100-nt region of homology

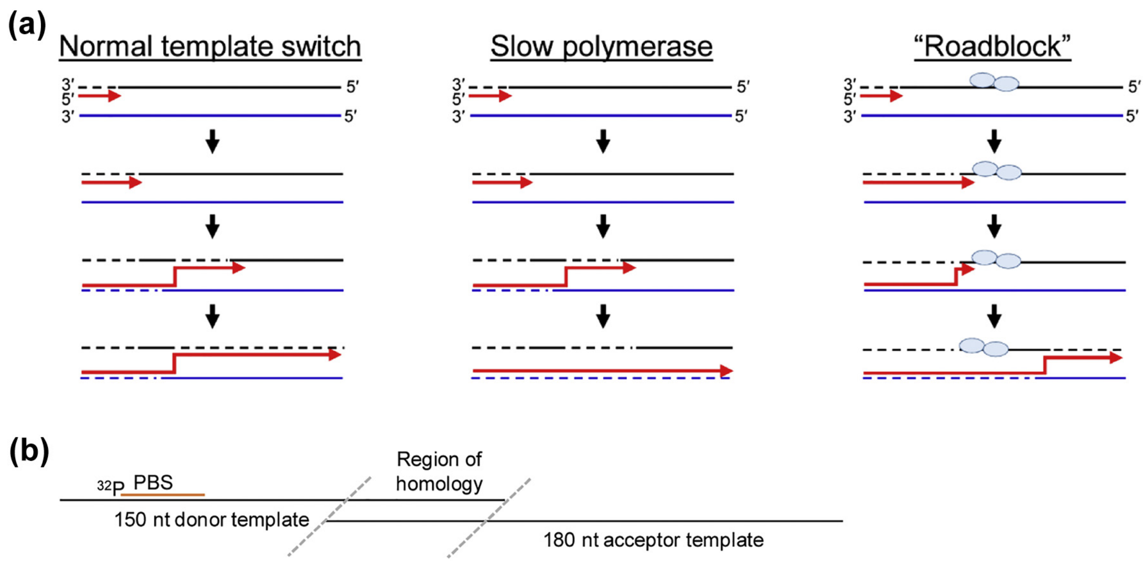

Fig. 1. Current models and schematic of template switching protocol. (a) Normal polymerase, slow polymerase (dynamic copy choice), and roadblock (forced copy choice) models of template switching (adapted from Hwang *et al.* [47] and Anderson et al. [59]). The black and blue lines represent RNA templates, whereas the red arrow indicates the newly synthesized DNA template. The hashed line indicates RNase H degradation of the RNA. In a template switch, the newly synthesized template can base pair with the second template (blue) and promote RT to template switch. The roadblock in the figure is an oligomer of an A3 enzyme. (b) Schematic of *in vitro* template switching assay substrates. A radiolabeled primer is annealed to the donor RNA template, which creates the primer/template. An acceptor template is included in the reaction that lacks the primer-binding site but has a region of homology with the donor template. Template switching from donor to acceptor template will generate a longer acceptor product after resolution by denaturing PAGE.

with the donor template as well as unique bases that allowed for a distinct acceptor product (Fig. 1b). If template switching occurred between the donor and the acceptor, the resulting complete product would be longer than that of the donor product alone. The A3:p/t ratios used were 0:1, 4:1, 8:1, and 32:1 (Fig. 2). The reactions also contained RT and nucleocapsid (NC) (see Materials and Methods). The NC was included in our *in vitro* reactions since the nucleic acid chaperone activity of NC is essential for strand transfer events in virions and A3 enzymes in virions would need to compete with NC to bind both RNA and (−) DNA [55].

We found that in the presence of increasing amounts of A3G, there was a reproducible, although not statistically significant, reduction in the amount of acceptor product at the 32:1 A3:p/t ratio. This indicated less template switching in the presence of A3G, compared to its absence, with the amount of acceptor product decreasing from 21% to 16% (Fig. 2a and e, compare 0:1 and 32:1 lanes). The slight decrease in acceptor product in the presence of A3G was also observable at the 8:1 ratio (Fig. 2a and Supplementary Fig. 1a). In contrast, we observed that the presence of high amounts of A3F promoted the formation of more acceptor product. Specifically, the template switching efficiency was increased from 29% to 90% (Fig. 2b and e, compare 0:1 and 32:1 lanes). Notably, this was accompanied by a strong pause band before the end of the donor template, consistent with the hypothesis that an A3 roadblock could promote template switching of RT (Fig. 2b). The A3F-induced increase in acceptor product was observable at the 8:1 ratio of A3F:p/t, although the change was not as significant as the 32:1 A3F:p/t ratio (Supplementary Fig. 1b, 0:1, 29%; 8:1, 35%). Altogether, the data demonstrated that A3G and A3F could affect RT template switching in different ways and that the effects of A3G and A3F on RT template switching primarily occurred at a high concentrations of A3 enzyme (32:1, Fig. 2a–b and e). Although the amount of A3F in virions is not known and the amount of A3G encapsidated in the presence or absence of Vif is highly variable [6,56], the high *in vitro* concentrations necessary to effect RT template switching are possible *in virio* where the capsid volume would result in a concentrating effect of proteins [32]. Nonetheless, the ability of A3F and A3G to bind ssDNA cooperatively and oligomerize would in itself create high local concentrations on the p/t [23,33] and is consistent with defective proviral DNA genomes in HIV+ individuals resulting primarily from insertions and deletions in comparison to those inactivated by A3-induced mutations [48]. We also examined two other A3s known to exert a deamination-independent mode of restriction, A3H and A3C I188. There was no observable effect on template switching by these two enzymes, suggesting that they are unlikely to modulate this function of RT (Fig. 2c–d, e, and Supplementary Fig. 1c–d).

Despite differences in the effects of individual A3 enzymes on RT template switching, all A3s tested

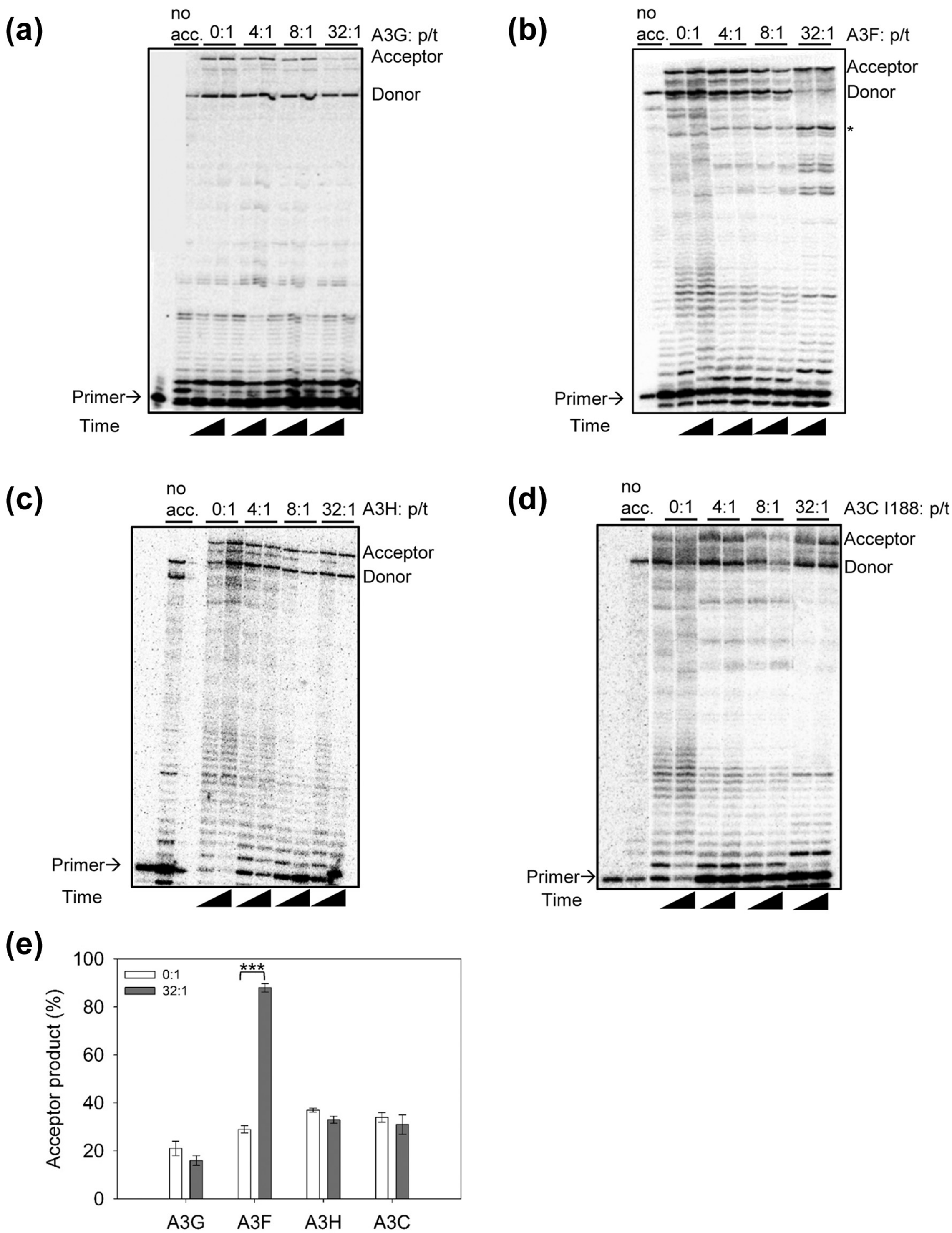

Fig. 2. Effect of A3s on the template switching efficiency of RT. Complete extension of the p/t (10 nM) results in a 150-nt donor product, whereas in the presence of acceptor, template switching results in the production of a longer acceptor product (Fig. 1b). (a–d) Extension of the p/t by 400 nM of RT in the absence (0:1) or presence (4:1, 8:1, 32:1) of (a) A3G, (b) A3F, (c) A3H, or (d) A3C I188. Reactions were sampled at 60 or 90 min. (e) Bar graph showing the quantified percentage of acceptor template at 90 min for 0:1 and 32:1 A3 to p/t. The gels shown in panels a–d are a representation from three independent experiments. Quantified results from the three independent experiments are summarized in panel e, with error bars representing the standard deviation from the mean. All conditions (0:1, 4:1, 8:1, 32:1) for all A3 enzymes are plotted in Supplemental Fig. 1. Designations for significant difference of values were as follows: ***$p \leq 0.001$, **$p \leq 0.01$, or *$p \leq 0.05$.

Table 1. Apparent dissociation constants (K_d) of HIV RT and A3 from the primer/template

Enzyme	K_d ± S.D.(nM)
HIV RT	500 ± 60
A3G	820 ± 100
A3F	100 ± 40
A3C I188	1840 ± 100
A3H	1300 ± 80
A3G NPM	200 ± 20
A3F NAM	230 ± 50

Data are summarized from Figs. 3 and 4 and are the average K_d from three independent experiments with the calculated standard deviation (S.D.) shown.

could induce pause sites to differing degrees during RT synthesis confirming that they were all able to interfere with DNA polymerization (Fig. 2a–d). Since A3 enzymes bind the p/t randomly, there were no common pause sites between experiments with different A3 enzymes, similar to what has been found in virions (Fig. 2a–d) [34]. However, for A3F that had significant effects on RT template switching, a distinct pause band increased in intensity with increasing A3F concentration (Fig. 2b, asterisk). It is likely that this region formed less secondary structure and provided a favorable single-stranded region for A3F to bind. That the intensity of this pause band increased with increasing amount of acceptor product being formed provides evidence for a relationship between an A3-induced road-block and RT template switching (Fig. 2b and e).

High affinity primer/template binding by A3F promotes HIV RT template switching

To determine why A3F was able to promote template switching, in contrast to the other tested A3s, we characterized how the A3 enzymes interacted with the p/t complex. Using rotational anisotropy, we determined the strength of the RT- and A3-p/t interaction. RT bound the p/t with an apparent dissociation constant (K_d) of 500 nM (Table 1). A3G bound the p/t with a K_d of 820 nM, which was 1.6-fold less than RT (Fig. 3a, Table 1). A3F bound the same p/t with an affinity 5-fold tighter than RT and ~8-fold tighter than A3G (Fig. 3b, Table 1; K_d of 100 nM). This suggests that the high affinity of A3F for the p/t induces more of a roadblock to RT than A3G and promotes increased template switching by slowing the polymerase. Consistent with this finding, A3H and A3C that had no

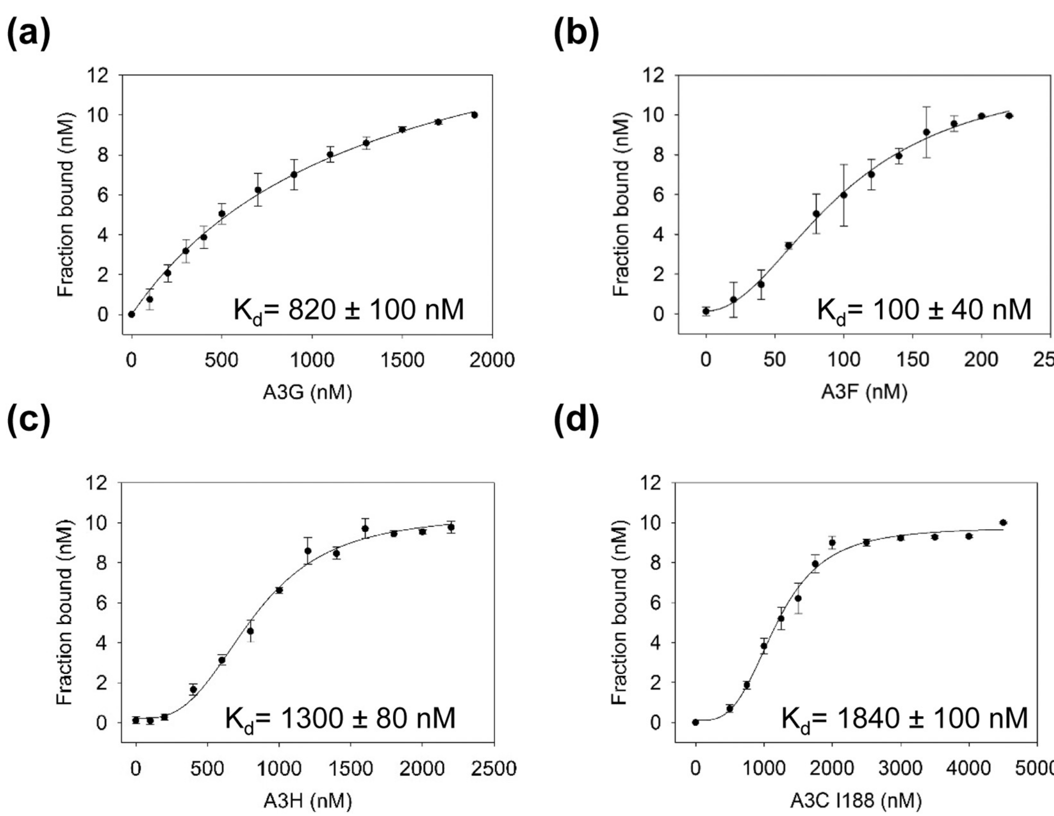

Fig. 3. Interaction of A3 with the primer/template. The K_d was determined by steady-state rotational anisotropy by titrating increasing amounts of (a) A3G, (b) A3F, (c) A3H, or (d) A3C I188 into a buffered solution containing 10 nM of fluorescently labeled p/t. The K_d and standard deviation from the mean are shown on the graph and summarized in Table 1. The results are the average of data from three independent experiments, and the error bars represent the standard deviation from the mean.

effect on RT template switching, both bound the p/t 2.6- to 3.7-fold less well than RT, 1.6- to 2-fold less well than A3G, and approximately 13- to 18-fold less well than A3F (Fig. 3c–d, Table 1).

To test further this rationale, we repeated the binding assays using a previously described mutant of A3G, which has a higher affinity for ssDNA, and a converse mutant in A3F, which interacts less well with ssDNA [23]. The A3G mutant (A3G NPM) has a 195NPM197 insertion in the connection loop between the N-terminal and C-terminal domains that was derived from the amino acid sequence of A3F. The NPM motif has been shown to impair A3F sliding movements on ssDNA, due to the tighter ssDNA binding [23]. The A3F mutant (A3F NAM) has a mutation at the proline at position 191 in the linker region, 190NAM192, and results in binding ssDNA with less affinity than wild-type A3F [23]. We used these mutants since they have been characterized previously and constitute the only full-length A3G or A3F mutants that can alter ssDNA binding without also disrupting oligomerization. We confirmed that these mutations changed the binding affinity as expected for the p/t used in this study (Fig. 4a–b, Table 1). The A3G NPM mutant bound the p/t 4-fold more tight than wild-type A3G (Fig. 4a, Table 1; K_d of 200 nM) and A3F NAM bound the p/t 2-fold less tight than wild-type A3F (Fig. 4b, Table 1; K_d of 230 nM). Both mutants bound the p/t ~2.5-fold more tight than RT (Fig. 4a–b, Table 1). To test whether strengthening the association of A3G with the p/t affected RT template switching, we tested the A3G NPM mutant using the *in vitro* template switching assay (Fig. 1b). In support of our hypothesis, the A3G NPM increased the amount of acceptor product compared to wild-type A3G, but 1.6-fold less efficiently than wild-type A3F (Fig. 4c and e). This can be attributed to the weaker binding to the p/t of A3G NPM compared to A3F (Table 1). This effect was also observed at the 8:1 A3G NPM:p/t ratio (Supplementary Fig. 1e). Furthermore, the appearance of more acceptor product correlated with increased intensity of a pause band unique to the reactions containing the A3G NPM (Fig. 4c) and similar to that observed for A3F (Fig. 2b). We observed 1.4-fold less acceptor product in the presence of A3F NAM compared to wild-type A3F, which correlates with the binding affinity for the p/t being 2-fold less than wild-type A3F (Fig. 4d and e, Table 1, and Supplementary Fig. 1f). We observed similar levels of template switching promotion for A3G NPM and A3F NAM, which correlated with the similar affinity of binding to the p/t by the mutants (Fig. 4, Table 1, and Supplementary Fig. 1e–f). Altogether, the data support the conclusion that a higher affinity for the p/t promotes template switching by RT.

Promotion of template switching in virions

To determine the extent to which these *in vitro* observations would influence template switching during a virus infection, we conducted single-cycle replication assays with a previously developed reporter virus system [57]. The system uses two HIV genomes from NL4–3 and HXB2 that both contain *gfp* with an inactivating mutation, which is transcribed from the *nef* open reading frame (Fig. 5a). The GFP fluorescence can only be detected if the mutations in a *gfp* are corrected through template switching (Fig. 5a). The viruses also have inactivating mutations in *vif*, *vpu*, *vpr*, and *env* and have been described in detail previously [57]. We cotransfected the plasmids for these two viruses into 293T cells with a VSV-G plasmid for pseudotyping and in the presence or absence of an A3F or A3G expression plasmid (Fig. 5a). Due to the known uracil based degradation of proviral DNA, we used catalytic mutants of A3F (E251Q) and A3G (E259Q) to minimize the degradation of proviral DNA, which would suppress the identification of potential template switching events [34]. Despite the lack of deamination, decreased integration of HIV proviral genomes can occur through entirely deamination-independent mechanisms based on the physical inhibition of RT that results in incomplete proviral DNAs being synthesized, preventing their integration into the host genome [36]. Consistent with these findings, qPCR for integrated HIV proviral DNA after cotransfection of both viral genomes demonstrated that both the A3F E251Q (A3F E/Q) and A3G E259Q (A3G E/Q) catalytic mutants were expressed in producer cells, encapsidiated into virions, and caused reduced proviral integration (Fig. 5b–c). The reduced proviral integration resulted in only 24% (A3F E/Q) or 45% (A3G E/Q) of integrated proviral DNA, relative to the no A3 condition (Fig. 5c). Accordingly, when we assessed for the level of GFP in the same population of viruses, which we could only detect if viral recombination through template switching had occurred (Fig. 5a), we observed that the A3F E/Q and A3G E/Q mutant conditions had less GFP containing cells than the No A3 condition (Fig. 5d). Since the overall decreased integration in the presence of A3F E/Q and A3G E/Q mutants would also decrease the apparent template switching that we could observe, we normalized the GFP data based on integration levels. In comparison to the no A3 condition, the normalization demonstrated that template switching occurred 2.3-fold more in the presence of A3F E/Q and 1.9-fold less in the presence of A3G E/Q (Fig. 5e). These data were consistent with the *in vitro* data showing that A3F could increase the frequency of RT template switching (Fig. 2b and e). The data also support that the small decrease in RT template switching frequency observed in the presence of A3G *in vitro* also occurred during virus replication (Fig. 2a and e). Altogether, these data support the conclusion that A3F and A3G can affect template switching in different ways during virus replication. The data further suggest that this effect is acting in addition to other deamination-independent mechanisms of HIV restriction.

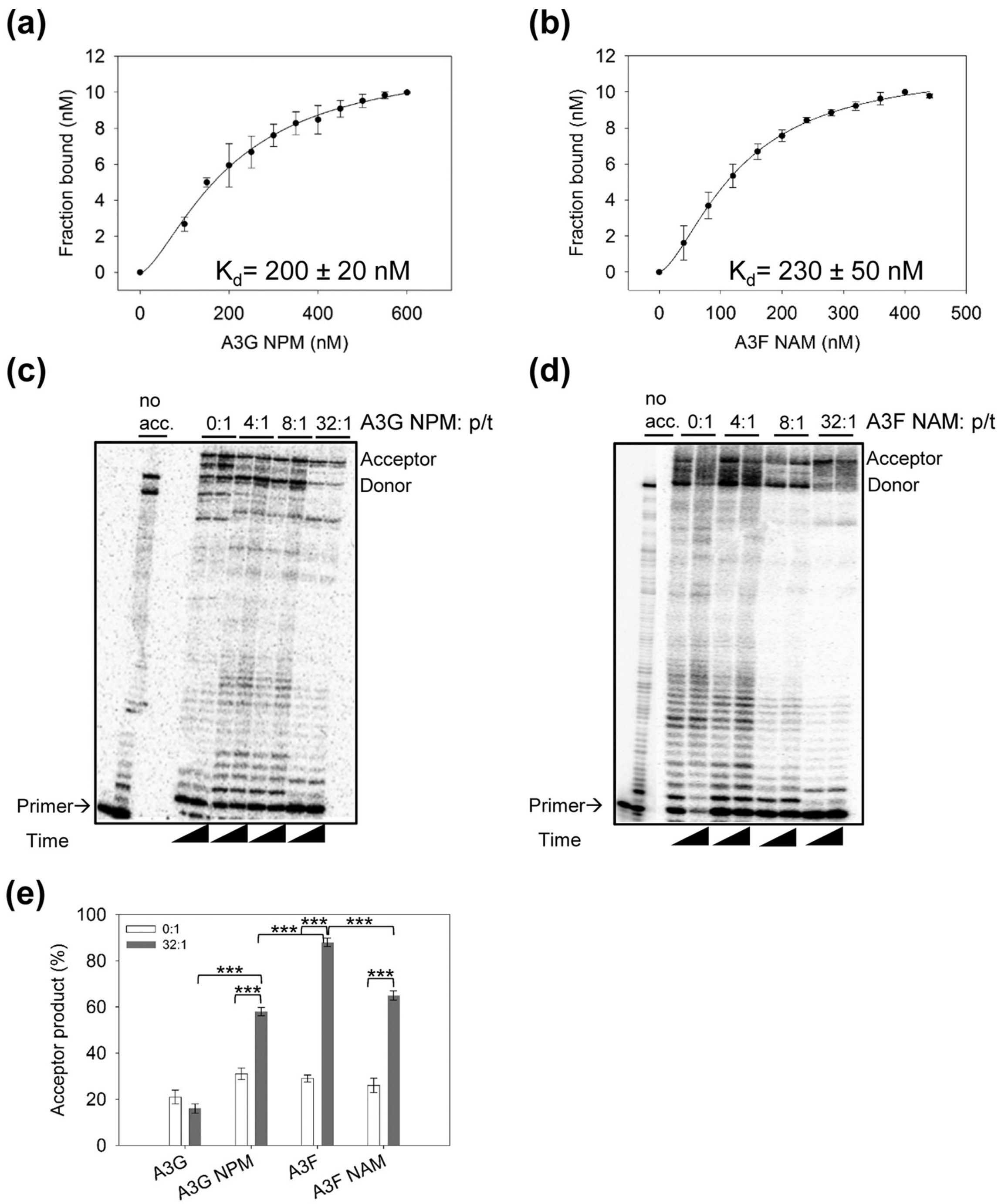

Fig. 4. Interaction of A3G NPM and A3F NAM with the primer/template and the effect on template switching. (a–b) The K_d was determined by steady-state rotational anisotropy by titrating increasing amounts of (a) A3G NPM or (b) A3F NAM with 10 nM of fluorescently labeled p/t. The K_d and standard deviation from the mean are shown on the graph and summarized in Table 1. The results are the average of data from three independent experiments, and the error bars represent the standard deviation from the mean. (c–d) Complete extension of the 10 nM p/t results in a 150-nt donor product, whereas in the presence of acceptor, template switching results in the production of a longer acceptor product. Extension of the p/t by 400 nM of RT in the absence (0:1) or presence (4:1, 8:1, 32:1) of (c) A3G NPM, or (d) A3F NAM. Reactions were sampled at 60 and 90 min. (e) Bar graph showing the quantified percent acceptor template at 90 min for 0:1 and 32:1 ratios of A3G and A3F wild type and mutants to p/t. The gels shown in panels c–d are a representation from three independent experiments. Quantified results from the three independent experiments are summarized in panel e, with error bars representing the standard deviation from the mean. The A3G and A3F results displayed are from Fig. 2e. All conditions (0:1, 4:1, 8:1, 32:1) for all A3G NPM and A3F NAM are plotted in Supplemental Fig. 1. Designations for significant difference of values were as follows: ***$p \leq 0.001$, **$p \leq 0.01$, or *$p \leq 0.05$.

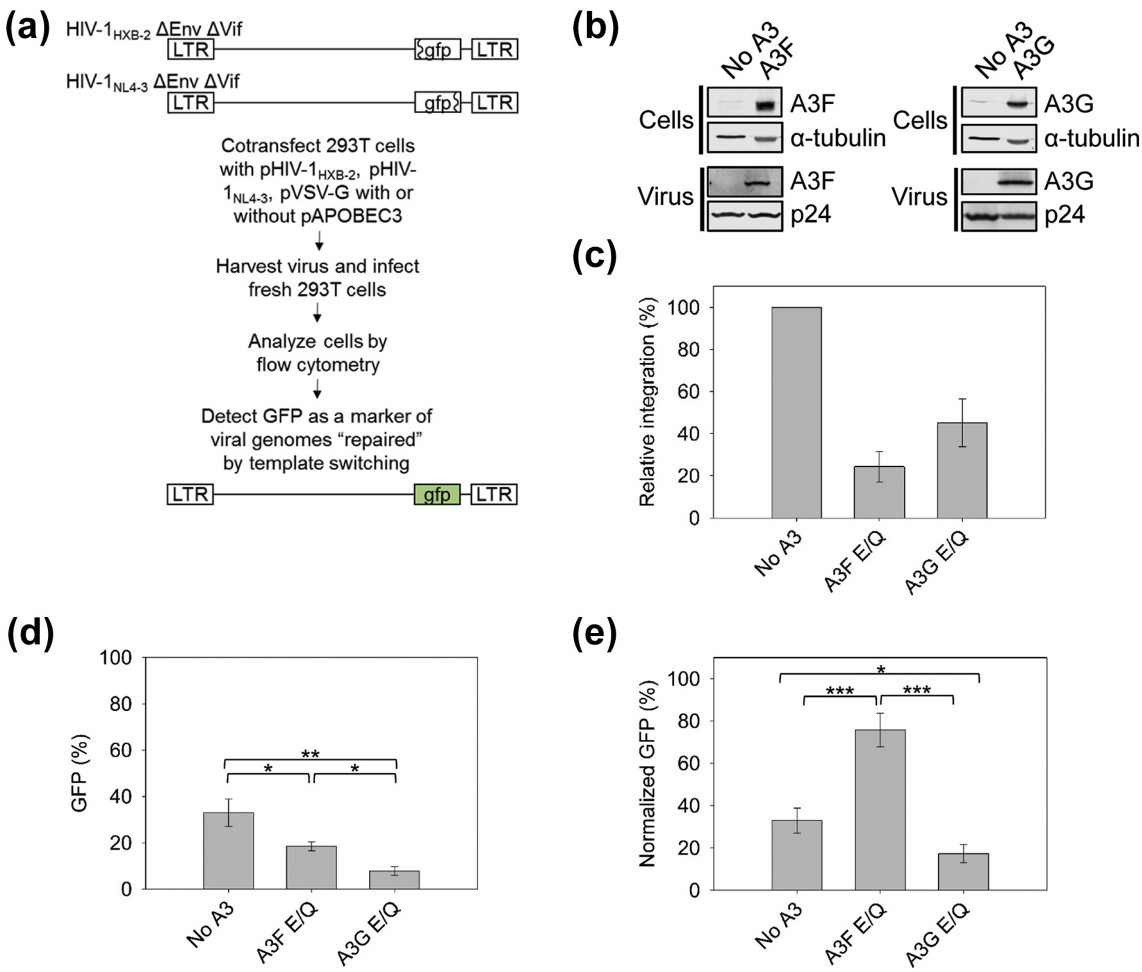

Fig. 5. Effects of A3F and A3G on proviral DNA integration and template switching in HIV infected cells. (a) The template switching events were detected by cotransfection of reporter HIV-1 constructs that had unique inactivating mutants in the gfp gene. Only through template switching and recombination could a functional gfp be produced. The effect of A3F E251Q-V5 (A3F E/Q) and A3G E259Q-HA (A3G E/Q) on the recombination events was assessed using this assay. The HIV-1 constructs were first reported in Ref. [57], from which the displayed graphic was also adapted. (b) Immunoblot of A3F E/Q and A3G E/Q demonstrating cellular expression and virion encapsidation. One representative blot from three independent experiments is shown. (c) The relative amount of proviral DNA integration in the presence of A3F E/Q and A3G E/Q to the No A3 condition was determined by qPCR. Both A3F E/Q and A3G E/Q could reduce proviral DNA integration. (d) Quantification of template switching through the detection of GFP, which can only be synthesized in cells that integrated a recombined HIV genome. When effects for integration are not used to normalize the GFP values, the A3F E/Q and A3G E/Q give an apparent decrease in template switching. (e) Considering results from panels c and d, the GFP values were normalized for integration effects and this resulted in normalized GFP values that demonstrated that A3F can increase and A3G can decrease template switching of RT. Quantified results from the three independent experiments are summarized in each panel with error bars representing the standard deviation from the mean. Designations for significant difference of values were $p \leq 0.001$ (***), $p \leq 0.01$(**), or $p \leq 0.05$ (*).

Discussion

A3 enzymes restrict viral replication through deamination-independent mechanisms in addition to the well-characterized deamination-dependent mechanism [27,29,32–34,36]. A3G and A3F delay the initiation of primer extension, which leads to production of fewer full-length extension products [25,28]. A3G and A3F are also able to inhibit the formation of late RT products by delaying DNA extension from the primer [28]. A3G has been found to interact with RT directly, which also leads to less full-length extension products being formed [25]. Although for human A3s and HIV these deamination-independent mechanisms complement the more dominant deamination-dependent restriction, for mouse A3, it has been found that a deamination-independent interaction with Moloney murine leukemia virus RT is primarily responsible for viral restriction [37]. Despite these findings, the deamination-independent mechanism of human A3 enzymes is poorly understood and characterized as a nonspecific effect. We sought to determine if the disruption of RT polymerase activity by these mechanisms had specific effects on RT, such as template switching. The data presented here extend our understanding of the effects of A3 enzymes on RT function. Namely, A3F uniquely promoted RT template switching (Figs. 2 and 5), and this was dependent on the high-affinity binding of A3F to the p/t (Fig. 3). A3G was the only A3 that could decrease template switching (Figs. 2 and 5). Since A3G can interact with RT directly [25,58], this may enable A3G to uniquely decrease RT template switching. Increases or decreases in template switching would disrupt the equilibrium of proviral DNA synthesis and can have detrimental effects on HIV replication [48,49].

The data obtained here are in agreement with reported mechanisms in previous studies regarding RT template switching. A previous study observed that when the polymerase activity was slowed through mutations within the polymerase domain, the frequency of template switching was increased [47]. This observed increase was due to increased RNase H cleavage behind the slow polymerase, which allowed for increased base pairing with the acceptor template (Fig. 1a, middle). Conversely, if there were mutations that affected the RNase H domain by decreasing RNase H cleavage, then less template was available for template switching and the rate of switching was reduced [47]. This dynamic copy choice model of template switching relies on the dynamics of RT and is in contrast to the forced copy choice model that posits that a roadblock to polymerization, such as a nick in the RNA template or a competitive binder, stalls the progression of the polymerase, and forces template switching (Fig. 1a, right) [59]. These two models of template switching are not mutually exclusive and have been shown to both contribute to efficient viral replication and genetic diversity [49]. However, excessive template switching can cause detrimental deletions or insertions [48,49]. We observed that an A3F bound to the template was able to force RT to switch templates by inducing a roadblock on the template (Figs. 1a, 2, and 5). The roadblock imposed by A3F on RT has not been studied in detail, in comparison to A3G [26,32,33]. For A3G, it has been determined that oligomerization is required for disruption of RT-mediated DNA synthesis [26,33,36]. However, it is known that A3F forms larger oligomers in solution than A3G, and that A3F oligomers are less dynamic than A3G oligomers [23,28]. For example, A3G oligomers are concentration dependent and larger oligomers form over time on ssDNA [23,33]. The more stable oligomers of A3F than A3G provides an additional possible explanation for why A3F would bind the p/t tighter and be able to impose a large enough roadblock to promote RT template switching as opposed to only inhibiting DNA synthesis.

Our *in vitro* experiments used an excess of acceptor template to promote template switching (Fig. 2). However, in virions, the two different viral genomes encapsidated in the confines of the virus particle are more likely to recombine through template switching despite their equimolar ratio, which we were able to observe (Fig. 5). This could lead to one of two outcomes: if intermolecular template switching occurs, this may promote recombination and virus evolution that could be beneficial to the virus or intramolecular switching may create regions of insertions and deletions that could inactivate the virus [45–49]. This may depend on the region where the template switching occurs. In our *in vitro* model, the template switching promoted by A3F occurred on RNA from the PBS region of the HIV genome, where the first template switch and strand transfer need to occur for proviral DNA synthesis [60]. Although this may suggest that A3F could promote proviral DNA synthesis, the strand transfers may occur prematurely as a result of A3F and disrupt synthesis of the (–) strand strong stop DNA. In addition, A3F promoted template switching in the cell-based assay, which used a region near the 3′-end of the genome as a reporter for template switching (Fig. 5a). As a result, the outcome may be context and region specific, similar to other situations, such as CTL escape, where A3s have been characterized to both help and hinder immune recognition [15,16,61].

Overall, this study has found that in addition to previously characterized roles of A3 enzymes to interfere with RT initiation of primer extension and processivity [25,27,32], some A3s are also able to modulate RT template switching. These deamination-independent mechanisms alone are not likely to cause similar levels of viral inhibition observed for cytosine deamination by A3s, and therefore are not as potent at restricting ΔVif HIV as the deamination-dependent mechanisms. However, in the presence of Vif, the additive effect of inhibiting RT processes and hypermutating viral DNA may ensure complete inactivation of HIV. This is consistent with the majority of integrated proviruses in HIV+ individuals being inactivated through deletions that likely resulted from template switching [48]. The delay in polymerization would also allow for a longer time for A3s to access and deaminate the viral DNA. Altogether, the multiple effects on RT, in addition to deamination of the viral (–) DNA, would cause higher levels of mutation to promote viral inactivation.

Materials and Methods

Synthesis of RNA templates

For the PBS RNA donor template, a 150-nt segment near the 5′-end of the HIV-1 genome (nt 521–676) encompassing the PBS and upstream region to the trans-activation response element site was PCR amplified. For the PBS RNA acceptor template, a 180-nt segment of the HIV-1 genome (451–635 nt) was PCR amplified. The PCR amplicons were cloned into the BamHI and EcoRI sites of the pSP72 vector (Promega). Sequences were amplified from the HIV-1 clone 93th253.3 (GenBank accession number U51189) [62]. The constructs were verified by sequencing. The RNA was synthesized *in vitro* by linearizing the vector at the BamHI site and using it as a T7 RNA polymerase substrate according to the manufacturer's instructions (Ambion Megascript kit). All primers and templates used are listed in Supplementary Table S1.

Protein expression and purification

Recombinant baculovirus for expression of GST-tagged NC, A3G, A3F, A3H, A3C I188, A3G NPM, and A3F NAM was constructed as described previously [18,23,24,63–65]. *Sf*9 cells were infected with recombinant A3 or NC expressing baculovirus at an MOI 1 for A3G and NC, MOI of 2 for A3F, MOI of 5 for A3C I188, and an MOI of 20 for A3H and were harvested after 72 h. Cells were lysed in the presence of RNase A and purified as described previously to obtain proteins cleaved from the GST tag [18,23,24,64,65]. NC, A3G, A3G NPM, and A3H were subjected to on-column cleavage from the GST tag with thrombin (GE Healthcare) at 21 °C for 18 h in thrombin digestion buffer [20 mM Hepes (pH 7.5), 150 mM NaCl, 10% glycerol, and 1 mM DTT]. A3F, A3C I188, and A3F NAM were eluted with the GST in elution buffer [100 mM Tris (pH 8.8), 150 mM NaCl, 10% (v/v) glycerol, and 50 mM reduced glutathione] digested with thrombin to cleave GST in solution for 6 h at 21 °C and then dialyzed [100 mM Tris (pH 7.5), 250 mM NaCl, 10% glycerol, and 1 mM DTT] overnight at 4 °C. To purify A3 enzymes from the free GST and thrombin, the enzyme stock was diluted to achieve a solution of 50 mM Tris (pH 7.5), 50 mM NaCl, 10% (v/v) glycerol, and 1 mM DTT for loading onto a DEAE FF column (GE Healthcare). Enzymes were eluted with a linear gradient of NaCl. The *Escherichia coli* strain containing the plasmid to express HIV RT p66/p51 was provided by Stuart Le Grice (National Cancer Institute). Expression and purification of HIV RT was carried out as previously described [66]. In brief, cell lysates produced using sonication were clarified by centrifugation and then purified using a HisTrap FF crude column (GE Healthcare) and HiTrap heparin HP (GE Healthcare) as described previously [66]. Protein fractions were stored at −80 °C. All proteins used were ~95% pure.

In vitro template switching assays

The 150-nt donor template RNA containing the PBS (nt 571–674) was heat annealed to an 18 nt ^{32}P-labeled RNA primer to mimic tRNA^{Lys,3} primer binding at nt 635–653. The p/t (10 nM) was then used in reactions containing RT buffer [50 mM Tris (pH 7.5), 40 mM KCl, 10 mM $MgCl_2$, 1 mM DTT), 500 μM deoxynucleotide triphosphates (dNTPs), 175 nM NC, 400 nM RT, and 400 nM acceptor RNA template for a 40:1 acceptor/donor ratio in the absence (0 nM) or presence of A3 (40, 80, or 320 nM) [67–69]. Reactions were preincubated at 37 °C for 1 min before the addition of dNTPs, which were used to start the reaction. A negative control was used, which contained all reaction components except RT to ensure that there was no contaminating polymerase activity. A second negative control was used, which contained all the reaction components except the acceptor RNA template to demonstrate the band pattern of the donor template alone. Reactions were stopped after 60 and 90 min by adding a 5-fold excess of 20 mM EDTA and 95% formamide. Template switching was visualized by resolving samples on a 16% denaturing 8 M urea polyacrylamide gel. Gel band intensities were measured by phosphorimaging with a Typhoon Trio multipurpose scanner (GE Healthcare). The integrated gel band intensities of all bands in a lane were calculated with ImageQuant software (GE Healthcare) and used to determine the relative amounts of donor *versus* acceptor products. Statistical significance of results was determined using a one-way random ANOVA.

Steady-state rotational anisotropy

Protein–p/t binding measurements were made by monitoring changes in steady-state fluorescence polarization (rotational anisotropy). For measuring binding to the p/t, a 5′-end fluorescein-labeled RNA primer that bound the PBS was heat annealed to the corresponding RNA template (PBS RNA) to form the binding substrate, as used in template switching assay. The rotational anisotropy experiments (60 μL) were incubated at 21 °C and contained RT buffer, p/t (10 nM) and increasing concentrations of RT or A3. Protein concentrations used ranged from 0 to 5 μM for measuring p/t binding affinities. Rotational anisotropy was measured with a QuantaMaster QM-4 fluorometer (Photon Technology International). Samples were excited with vertically polarized light at 495 nm (6-nm band pass), and both vertical and horizontal emissions were monitored at 520 nm (6-nm band pass). The K_d values were determined through regression analysis using Sigma Plot 11.2 software.

Cell-based template switching assay

The HIV vectors used for the template switching assay were kindly provided by Wei-Shau Hu (National Cancer Institute) and have been previously described [57]. The vectors, which are based on either HIV-1 HXB2 or NL43, each contain a *gfp* with a unique inactivating mutation that is expressed from the *nef* open reading frame [57]. Only through using a 588-nt homology region with in the *gfp* genes for template switching can the wild-type GFP be expressed [57]. To use these vectors to determine the frequency of template switching, equal amounts of each vector (400 ng) were transfected into 3×10^5 293T cells grown with DMEM and 10% FBS in a 6-well plate with 200 ng pVSV-G and a pVIVO2 plasmid (50 ng) that was empty or expressed A3F E251Q-V5 or A3G E259Q-HA. Cloning of the A3 constructs in pVIVO2 has been previously described [28]. The day after the transfection, the media was changed and 24 h after the media change the virus was harvested and clarified by filtering through a 0.45-μm PVDF syringe filter. The virus was then titered on TZM-Bl cells and equal amounts of virus (MOI < 1) were used to infect 5×10^4 293T cells in a 24-well plate in the presence of polybrene (8 μg/mL). The day after infection, the media was changed, and 16 h after the media change, the cells were harvested and fixed for analysis by flow cytometry. The GFP signal was detected using a Beckman CytoFLEX Flow Cytometer. Statistical significance of results was determined using a one-way random ANOVA.

Proviral DNA integration assay

Methods to quantify the integrated proviral DNA were adapted from previous publications [36,70,71]. For infections, 1×10^5 293T cells per well of a 12-well plate were infected by spinoculation (1 h at 800*g*) and in the presence of polybrene (8 μg/mL) with HIV produced from the cell-based template switching assay. DNA was extracted after 24 h using DNazol according to the manufacturer's instructions. The DNA was then treated with DpnI, and 50 ng was used in a PCR with primers qAlu1 and qAlu2 [36] and Nef FWD-OUT (5′GGG TCA GAT ATC CAC TGA CCT TTG G) to ensure amplification of DNA from integrated HIV genomes. The PCR cycle used a Taq Master Mix (Qiagen) and an annealing temperature of 50 °C and extension time of 3 min. The PCR was then diluted 40-fold and used as the template in a qPCR with 9 pmol/mL of each primer (Primer 1, 5′GTA CCA GTT GAG CCA GAT AAG G; Primer 2, 5′GCT GTC AA ACCT CCA CTC TAA C) and 0.25 pmol/mL of the probe (5′FAM-TGT TAC ACC -ZEN- CTG TGA AGC CTG CAT-IABkFQ). Reactions were performed in triplicate with TaqMan Gene Expression master mix (Applied Biosystems). Cycling conditions were 10 min at 95 °C, followed by 40 cycles of 15 s at 95 °C and 1 min at 60 °C using a Bio-Rad CFX-96. The copy numbers in each sample were normalized for DNA input using human RNase P (Applied Biosystems).

Immunoblotting

Tagged A3 enzymes (50 ng pVIVO2 plasmid transfected) in cells or virions were detected by mouse anti-HA (A3G, 1:1000; Sigma) or rabbit anti-V5 (A3F, 1:500; Sigma). Mouse or rabbit anti-α-tubulin (1:1000; Sigma) and mouse anti-p24 (1:1000, cat. no. 3537; NIH AIDS Reagent Program) were used to detect the cell lysate loading control (α-tubulin) and the virus lysate loading control (p24) [72,73]. Secondary detection was performed using Licor IRDye antibodies produced in goat (IRDye 680-labeled anti-rabbit and IRDye 800-labeled anti mouse). For cell lysates, 30 μg total protein was used. For virions, a portion of the filtered supernatant was concentrated using Retro-X concentrator (Clonetech) according to the manufacturer's instructions, and 15 μL was used.

Supplementary data to this article can be found online at https://doi.org/10.1016/j.jmb.2019.02.015.

Acknowledgments

We thank Wojciech Dawicki and Mark Boyd for assistance with flow cytometry and Robin P. Love for assistance with immunoblotting. The following reagents were obtained through the NIH AIDS Reagent Program, Division of AIDS, NIAID, NIH: HIV-1 clone p93th253.3 from Dr. Feng Gao and Dr. Beatrice Hahn, and anti-HIV-1 p24 Monoclonal (183-H12-5C) (cat. no. 3537) from Dr. Bruce Chesebro and Kathy Wehrly. This study was supported by a Canadian Institutes of Health Research grant (MOP-137090) to L.C.

Received 8 January 2019;
Received in revised form 14 February 2019;
Accepted 15 February 2019
Available online 22 February 2019

Keywords:
enzyme–DNA interactions;
DNA synthesis;
proviral DNA integration;
retroviral recombination;
polymerase

Abbreviations used:
A3, APOBEC3; HIV, human immunodeficiency virus type 1; Vif, viral infectivity factor; ss, single-stranded; RT, reverse transcriptase; PBS, primer binding site; p/t, primer/template; K_d, apparent dissociation constant; dNTP, deoxynucleotide triphosphate; NC, nucleocapsid.

References

[1] M.B. Adolph, R.P. Love, L. Chelico, Biochemical basis of APOBEC3 deoxycytidine deaminase activity on diverse DNA substrates, ACS Infect. Dis. 4 (2018) 224–238.
[2] J.D. Salter, H.C. Smith, Modeling the embrace of a Mutator: APOBEC selection of nucleic acid ligands, Trends Biochem. Sci. 43 (2018) 606–622.
[3] R.S. Harris, J.F. Hultquist, D.T. Evans, The restriction factors of human immunodeficiency virus, J. Biol. Chem. 287 (2012) 40875–40883.

[4] A.M. Sheehy, N.C. Gaddis, J.D. Choi, M.H. Malim, Isolation of a human gene that inhibits HIV-1 infection and is suppressed by the viral Vif protein, Nature. 418 (2002) 646–650.
[5] N. Mohammadzadeh, T.B. Follack, R.P. Love, K. Stewart, S. Sanche, L. Chelico, Polymorphisms of the cytidine deaminase APOBEC3F have different HIV-1 restriction efficiencies, Virology. 527 (2019) 21–31.
[6] R. Nowarski, E. Britan-Rosich, T. Shiloach, M. Kotler, Hypermutation by intersegmental transfer of APOBEC3G cytidine deaminase, Nat. Struct. Mol. Biol. 15 (2008) 1059–1066.
[7] R. Suspene, P. Sommer, M. Henry, S. Ferris, D. Guetard, S. Pochet, et al., APOBEC3G is a single-stranded DNA cytidine deaminase and functions independently of HIV reverse transcriptase, Nucleic Acids Res. 32 (2004) 2421–2429.
[8] Q. Yu, R. Konig, S. Pillai, K. Chiles, M. Kearney, S. Palmer, et al., Single-strand specificity of APOBEC3G accounts for minus-strand deamination of the HIV genome, Nat. Struct. Mol. Biol. 11 (2004) 435–442.
[9] R.S. Harris, K.N. Bishop, A.M. Sheehy, H.M. Craig, S.K. Petersen-Mahrt, I.N. Watt, et al., DNA deamination mediates innate immunity to retroviral infection, Cell. 113 (2003) 803–809.
[10] B. Mangeat, P. Turelli, G. Caron, M. Friedli, L. Perrin, D. Trono, Broad antiretroviral defence by human APOBEC3G through lethal editing of nascent reverse transcripts, Nature. 424 (2003) 99–103.
[11] H. Zhang, B. Yang, R.J. Pomerantz, C. Zhang, S.C. Arunachalam, L. Gao, The cytidine deaminase CEM15 induces hypermutation in newly synthesized HIV-1 DNA, Nature. 424 (2003) 94–98.
[12] L.C. Mulder, A. Harari, V. Simon, Cytidine deamination induced HIV-1 drug resistance, Proc. Natl. Acad. Sci. U. S. A. 105 (2008) 5501–5506.
[13] E.Y. Kim, T. Bhattacharya, K. Kunstman, P. Swantek, F.A. Koning, M.H. Malim, et al., Human APOBEC3G-mediated editing can promote HIV-1 sequence diversification and accelerate adaptation to selective pressure, J. Virol. 84 (2010) 10402–10405.
[14] E.Y. Kim, R. Lorenzo-Redondo, S.J. Little, Y.S. Chung, P.K. Phalora, I. Maljkovic Berry, et al., Human APOBEC3 induced mutation of human immunodeficiency virus type-1 contributes to adaptation and evolution in natural infection, PLoS Pathog. 10 (2014), e1004281.
[15] M. Monajemi, C.F. Woodworth, K. Zipperlen, M. Gallant, M.D. Grant, M. Larijani, Positioning of APOBEC3G/F mutational hotspots in the human immunodeficiency virus genome favors reduced recognition by CD8+ T cells, PLoS One 9 (2014), e93428.
[16] K.D. Squires, M. Monajemi, C.F. Woodworth, M.D. Grant, M. Larijani, Impact of APOBEC mutations on CD8+ T cell recognition of HIV epitopes varies depending on the restricting HLA, J. Acquir. Immune Defic. Syndr. 70 (2015) 172–178.
[17] Y. Feng, T.T. Baig, R.P. Love, L. Chelico, Suppression of APOBEC3-mediated restriction of HIV-1 by Vif, Front. Microbiol. 5 (2014) 450.
[18] M.B. Adolph, A. Ara, Y. Feng, C.J. Wittkopp, M. Emerman, J. S. Fraser, et al., Cytidine deaminase efficiency of the lentiviral viral restriction factor APOBEC3C correlates with dimerization, Nucleic Acids Res. 45 (2017) 3378–3394.
[19] C.J. Wittkopp, M.B. Adolph, L.I. Wu, L. Chelico, M. Emerman, A single nucleotide polymorphism in human APOBEC3C enhances restriction of lentiviruses, PLoS Pathog. 12 (2016), e1005865.
[20] V.B. Soros, W. Yonemoto, W.C. Greene, Newly synthesized APOBEC3G is incorporated into HIV virions, inhibited by HIV RNA, and subsequently activated by RNase H, PLoS Pathog. 3 (2007), e15.
[21] O.G. Berg, R.B. Winter, P.H. von Hippel, Diffusion-driven mechanisms of protein translocation on nucleic acids. 1. Models and theory, Biochemistry. 20 (1981) 6929–6948.
[22] P.H. von Hippel, O.G. Berg, Facilitated target location in biological systems, J. Biol. Chem. 264 (1989) 675–678.
[23] A. Ara, R.P. Love, L. Chelico, Different mutagenic potential of HIV-1 restriction factors APOBEC3G and APOBEC3F is determined by distinct single-stranded DNA scanning mechanisms, PLoS Pathog. 10 (2014), e1004024.
[24] Y. Feng, R.P. Love, A. Ara, T.T. Baig, M.B. Adolph, L. Chelico, Natural polymorphisms and oligomerization of human APOBEC3H contribute to single-stranded DNA scanning ability, J. Biol. Chem. 290 (2015) 27188–27203.
[25] M.B. Adolph, J. Webb, L. Chelico, Retroviral restriction factor APOBEC3G delays the initiation of DNA synthesis by HIV-1 reverse transcriptase, PLoS One 8 (2013), e64196.
[26] K.R. Chaurasiya, M.J. McCauley, W. Wang, D.F. Qualley, T. Wu, S. Kitamura, et al., Oligomerization transforms human APOBEC3G from an efficient enzyme to a slowly dissociating nucleic acid-binding protein, Nat. Chem. 6 (2014) 28–33.
[27] K. Gillick, D. Pollpeter, P. Phalora, E.Y. Kim, S.M. Wolinsky, M. H. Malim, Suppression of HIV-1 infection by APOBEC3 proteins in primary human CD4(+) T cells is associated with inhibition of processive reverse transcription as well as excessive cytidine deamination, J. Virol. 87 (2013) 1508–1517.
[28] A. Ara, R.P. Love, T.B. Follack, K.A. Ahmed, M.B. Adolph, L. Chelico, Mechanism of enhanced HIV restriction by virion coencapsidated cytidine deaminases APOBEC3F and APOBEC3G, J. Virol. 91 (2017).
[29] K.N. Bishop, M. Verma, E.Y. Kim, S.M. Wolinsky, M.H. Malim, APOBEC3G inhibits elongation of HIV-1 reverse transcripts, PLoS Pathog. 4 (2008), e1000231.
[30] X.Y. Li, F. Guo, L. Zhang, L. Kleiman, S. Cen, APOBEC3G inhibits DNA strand transfer during HIV-1 reverse transcription, J. Biol. Chem. 282 (2007) 32065–32074.
[31] X. Wang, Z. Ao, L. Chen, G. Kobinger, J. Peng, X. Yao, The cellular antiviral protein APOBEC3G interacts with HIV-1 reverse transcriptase and inhibits its function during viral replication, J. Virol. 86 (2012) 3777–3786.
[32] Y. Iwatani, D.S. Chan, F. Wang, K.S. Maynard, W. Sugiura, A.M. Gronenborn, et al., Deaminase-independent inhibition of HIV-1 reverse transcription by APOBEC3G, Nucleic Acids Res. 35 (2007) 7096–7108.
[33] M. Morse, R. Huo, Y. Feng, I. Rouzina, L. Chelico, M.C. Williams, Dimerization regulates both deaminase-dependent and deaminase-independent HIV-1 restriction by APOBEC3G, Nat. Commun. 8 (2017) 597.
[34] D. Pollpeter, M. Parsons, A.E. Sobala, S. Coxhead, R.D. Lang, A.M. Bruns, et al., Deep sequencing of HIV-1 reverse transcripts reveals the multifaceted antiviral functions of APOBEC3G, Nat. Microbiol. 3 (2018) 220–233.
[35] R.K. Holmes, F.A. Koning, K.N. Bishop, M.H. Malim, APOBEC3F can inhibit the accumulation of HIV-1 reverse transcription products in the absence of hypermutation. Comparisons with APOBEC3G, J. Biol. Chem. 282 (2007) 2587–2595.
[36] K. Belanger, M. Savoie, M.C. Rosales Gerpe, J.F. Couture, M.A. Langlois, Binding of RNA by APOBEC3G controls

deamination-independent restriction of retroviruses, Nucleic Acids Res. 41 (2013) 7438–7452.
[37] S. Stavrou, W. Zhao, K. Blouch, S.R. Ross, Deaminase-dead mouse APOBEC3 is an in vivo retroviral restriction factor, J. Virol. 92 (2018).
[38] H.M. Temin, Retrovirus variation and reverse transcription: abnormal strand transfers result in retrovirus genetic variation, Proc. Natl. Acad. Sci. U. S. A. 90 (1993) 6900–6903.
[39] V.P. Basu, M. Song, L. Gao, S.T. Rigby, M.N. Hanson, R.A. Bambara, Strand transfer events during HIV-1 reverse transcription, Virus Res. 134 (2008) 19–38.
[40] P.E. Johnson, R.B. Turner, Z.R. Wu, L. Hairston, J. Guo, J.G. Levin, et al., A mechanism for plus-strand transfer enhancement by the HIV-1 nucleocapsid protein during reverse transcription, Biochemistry. 39 (2000) 9084–9091.
[41] R.A. Katz, A.M. Skalka, Generation of diversity in retroviruses, Annu. Rev. Genet. 24 (1990) 409–445.
[42] W.S. Hu, H.M. Temin, Retroviral recombination and reverse transcription, Science. 250 (1990) 1227–1233.
[43] W.S. Hu, E.H. Bowman, K.A. Delviks, V.K. Pathak, Homologous recombination occurs in a distinct retroviral subpopulation and exhibits high negative interference, J. Virol. 71 (1997) 6028–6036.
[44] J. Zhang, H.M. Temin, Rate and mechanism of nonhomologous recombination during a single cycle of retroviral replication, Science. 259 (1993) 234–238.
[45] S. Parthasarathi, A. Varela-Echavarría, Y. Ron, B.D. Preston, J.P. Dougherty, Genetic rearrangements occurring during a single cycle of murine leukemia virus vector replication: characterization and implications, J. Virol. 69 (1995) 7991–8000.
[46] V.K. Pathak, H.M. Temin, Broad spectrum of in vivo forward mutations, hypermutations, and mutational hotspots in a retroviral shuttle vector after a single replication cycle: substitutions, frameshifts, and hypermutations, Proc. Natl. Acad. Sci. U. S. A. 87 (1990) 6019–6023.
[47] C.K. Hwang, E.S. Svarovskaia, V.K. Pathak, Dynamic copy choice: steady state between murine leukemia virus polymerase and polymerase-dependent RNase H activity determines frequency of in vivo template switching, Proc. Natl. Acad. Sci. U. S. A. 98 (2001) 12209–12214.
[48] K.M. Bruner, A.J. Murray, R.A. Pollack, M.G. Soliman, S.B. Laskey, A.A. Capoferri, et al., Defective proviruses rapidly accumulate during acute HIV-1 infection, Nat. Med. 22 (2016) 1043–1049.
[49] J.M.O. Rawson, O.A. Nikolaitchik, B.F. Keele, V.K. Pathak, W.S. Hu, Recombination is required for efficient HIV-1 replication and the maintenance of viral genome integrity, Nucleic Acids Res. 46 (2018) 10535–10545.
[50] B.C. Ramirez, E. Simon-Loriere, R. Galetto, M. Negroni, Implications of recombination for HIV diversity, Virus Res. 134 (2008) 64–73.
[51] J.F. Hultquist, J.A. Lengyel, E.W. Refsland, R.S. LaRue, L. Lackey, W.L. Brown, et al., Human and rhesus APOBEC3D, APOBEC3F, APOBEC3G, and APOBEC3H demonstrate a conserved capacity to restrict Vif-deficient HIV-1, J. Virol. 85 (2011) 11220–11234.
[52] B.D. Anderson, T. Ikeda, S.A. Moghadasi, A.S. Martin, W.L. Brown, R.S. Harris, Natural APOBEC3C variants can elicit differential HIV-1 restriction activity, Retrovirology. 15 (2018) 78.
[53] S. Liu, E.A. Abbondanzieri, J.W. Rausch, S.F. Le Grice, X. Zhuang, Slide into action: dynamic shuttling of HIV reverse transcriptase on nucleic acid substrates, Science. 322 (2008) 1092–1097.
[54] S. Liu, B.T. Harada, J.T. Miller, S.F. Le Grice, X. Zhuang, Initiation complex dynamics direct the transitions between distinct phases of early HIV reverse transcription, Nat. Struct. Mol. Biol. 17 (2010) 1453–1460.
[55] B. Rene, O. Mauffret, P. Fosse, Retroviral nucleocapsid proteins and DNA strand transfers, Biochim. Open 7 (2018) 10–25.
[56] H. Xu, E. Chertova, J. Chen, D.E. Ott, J.D. Roser, W.S. Hu, et al., Stoichiometry of the antiviral protein APOBEC3G in HIV-1 virions, Virology. 360 (2007) 247–256.
[57] K.A. Delviks-Frankenberry, O.A. Nikolaitchik, R.C. Burdick, R.J. Gorelick, B.F. Keele, W.S. Hu, et al., Minimal contribution of APOBEC3-induced G-to-A Hypermutation to HIV-1 recombination and genetic variation, PLoS Pathog. 12 (2016), e1005646.
[58] M.H. Malim, APOBEC proteins and intrinsic resistance to HIV-1 infection, Philos. Trans. R. Soc. Lond. Ser. B Biol. Sci. 364 (2009) 675–687.
[59] J.A. Anderson, R.J. Teufel, P.D. Yin, W.S. Hu, Correlated template-switching events during minus-strand DNA synthesis: a mechanism for high negative interference during retroviral recombination, J. Virol. 72 (1998) 1186–1194.
[60] J.M. Coffin, S.H. Hughes, H.E. Varmus, Retroviruses, Cold Spring Harbor Laboratory Press, Cold Spring Harbor, New York, 1997.
[61] R.A. Pollack, R.B. Jones, M. Pertea, K.M. Bruner, A.R. Martin, A.S. Thomas, et al., Defective HIV-1 Proviruses Are Expressed and Can Be Recognized by Cytotoxic T Lymphocytes, which Shape the Proviral Landscape, Cell Host Microbe 21 (2017) 494-506.e4.
[62] F. Gao, D.L. Robertson, S.G. Morrison, H. Hui, S. Craig, J. Decker, et al., The heterosexual human immunodeficiency virus type 1 epidemic in Thailand is caused by an intersubtype (A/E) recombinant of African origin, J. Virol. 70 (1996) 7013–7029.
[63] L. Chelico, P. Pham, P. Calabrese, M.F. Goodman, APOBEC3G DNA deaminase acts processively $3' \rightarrow 5'$ on single-stranded DNA, Nat. Struct. Mol. Biol. 13 (2006) 392–399.
[64] L. Chelico, C. Prochnow, D.A. Erie, X.S. Chen, M.F. Goodman, Structural model for deoxycytidine deamination mechanisms of the HIV-1 inactivation enzyme APOBEC3G, J. Biol. Chem. 285 (2010) 16195–16205.
[65] Y. Feng, L. Chelico, Intensity of deoxycytidine deamination of HIV-1 proviral DNA by the retroviral restriction factor APOBEC3G is mediated by the noncatalytic domain, J. Biol. Chem. 286 (2011) 11415–11426.
[66] S.F. Le Grice, F. Gruninger-Leitch, Rapid purification of homodimer and heterodimer HIV-1 reverse transcriptase by metal chelate affinity chromatography, Eur. J. Biochem. 187 (1990) 307–314.
[67] E.J. Arts, X. Li, Z. Gu, L. Kleiman, M.A. Parniak, M.A. Wainberg, Comparison of deoxyoligonucleotide and tRNA (Lys-3) as primers in an endogenous human immunodeficiency virus-1 in vitro reverse transcription/template-switching reaction, J. Biol. Chem. 269 (1994) 14672–14680.
[68] E.J. Arts, M.A. Wainberg, Preferential incorporation of nucleoside analogs after template switching during human immunodeficiency virus reverse transcription, Antimicrob. Agents Chemother. 38 (1994) 1008–1016.
[69] E.J. Arts, Z. Li, M.A. Wainberg, Analysis of primer extension and the first template switch during human immunodeficiency virus reverse transcription, J. Biomed. Sci. 2 (1995) 314–321.

[70] S.L. Butler, M.S. Hansen, F.D. Bushman, A quantitative assay for HIV DNA integration in vivo, Nat. Med. 7 (2001) 631–634.
[71] A. Brussel, O. Delelis, P. Sonigo, Alu-LTR real-time nested PCR assay for quantifying integrated HIV-1 DNA, Methods Mol. Biol. 304 (2005) 139–154.
[72] K. Toohey, K. Wehrly, J. Nishio, S. Perryman, B. Chesebro, Human immunodeficiency virus envelope V1 and V2 regions influence replication efficiency in macrophages by affecting virus spread, Virology. 213 (1995) 70–79.
[73] K. Wehrly, B. Chesebro, p24 antigen capture assay for quantification of human immunodeficiency virus using readily available inexpensive reagents, Methods. 12 (1997) 288–293.